Published OnlineFirst January 12, 2012; DOI:10.1158/1078-0432.CCR-11-2725

The histologic characteristics of surgically resected specimens, which were diagnosed as serous histologic type by 2 pathologists at each institute, were at first assessed on formalin-fixed and paraffin-embedded hematoxylin and eosin sections by 8 gynecologic pathologists who belong to Department of Pathology in 4 institutes (Niigata University, National Defense Medical Collage, Tottori University, Kagoshima City Hospital). Next, these sections were reviewed under central pathologic review by 2 independent gynecologic pathologists (H.T. and T.M.) with no knowledge of patients' clinical data. Histologic subtype was diagnosed based on WHO classification of ovarian tumors (17). The degree of histologic differentiation is determined according to Silverberg classification (18).

Microarray experiments

Frozen tissues containing more than 70% tumor cells upon histologic evaluation were used for RNA extraction. Total RNA was extracted from tissue samples as previously described (19). Five hundred nanograms of total RNA was converted into labeled cRNA with nucleotides coupled to a cyanine 3-CTP (Cy3; PerkinElmer) using the Quick Amp Labeling Kit, one-color (Agilent Technologies). Cy3-labeled cRNA (1.65 μg) was hybridized for 17 hours at 65°C to an Agilent Whole Human Genome Oligo Microarray (G4112F), which carries 60-mer probes to more than 40,000 human transcripts. The hybridized microarray was washed and then scanned in Cy3 channel with the Agilent DNA Microarray Scanner [model G2565CA, $n = 260$ (Japanese data set A); G2565AA, $n = 40$ (Japanese data set B)]. Signal intensity per spot was generated from the scanned image with Feature Extraction Software (version 10.1, Japanese data set A; version 9.1, Japanese data set B; Agilent Technologies) with default settings. Spots that did not pass quality control procedures were flagged as "Not Detected."

Next, we obtained Affymetrix HG-U133Plus2.0 microarray (Affymetrix) data from 10 ovarian cancer samples that had been already been analyzed by the Agilent Whole Human Genome Oligo Microarray. Ten ovarian cancer samples were randomly selected from 260 samples in the Japanese data set A. Microarray experiments were carried out according to the Affymetrix-recommended protocols. Briefly, biotinylated cRNAs were synthesized by GeneChip 3'IVT Express Kit (Affymetrix) from 250 ng total RNA according to the manufacturer's instructions. Biotinylated cRNA yield were checked with the NanoDrop ND-1000 Spectrophotometer. Following fragmentation, 10 μg of cRNA were hybridized for 16 hours at 45°C on GeneChip Human Genome U133 Plus 2.0 Array. GeneChips were washed and stained in the Affymetrix Fluidics Station 450, and scanned with GeneChip Scanner 3000 7G.

The MIAME-compliant microarray data were deposited into the Gene Expression Omnibus data repository (accession number GSE32062 and GSE32063).

Microarray data analysis

We prepared 2 our microarray data sets [Japanese data set A ($n = 260$) and B ($n = 40$)] and 4 publicly available large sample-sized ($n > 100$) microarray data sets [TCGA data set (http://tcga-data.nci.nih.gov/tcga/tcgaHome2.jsp; ref. 11), Tothill's data set (GSE9891; ref. 12), Bonome's data set (GSE26712; ref. 13), and Dressman's data set (14)] to discover predictive biomarkers. Clinical information of publicly available microarray data sets was obtained from their articles and websites. From Tothill's original data set ($n = 285$), we selected 131 samples that (i) were diagnosed as advanced stage serous adenocarcinoma, (ii) were treated by platinum/taxane–based chemotherapy, and (iii) have clinical data about onset age, stage, grade, surgery, and survival time. Publicly available clinical information in TCGA was downloaded from TCGA Data portal (http://tcga-data.nci.nih.gov/tcga/tcgaHome2.jsp) at June 25, 2011. By the same methods above, 319 samples were selected from 562 microarray data as TCGA data set (Affymetrix HT-HG-U133A). In this study, patients who were treated by adjuvant chemotherapy including molecular-targeted agents were excluded.

On the Agilent platform, data normalization was carried out in GeneSpring GX 11.5 (Agilent Technologies) as follows: (i) threshold raw signals were set to 1.0 and (ii) 75th percentile normalization. Affymetrix microarray data were normalized and summarized with robust multiple average in GeneSpring GX 11.5 (Agilent Technologies). To compare the microarray data sets measured with 4 different platforms (Agilent Whole Human Genome Oligo Microarray, Affymetrix HG-U133A, HG-U133Plus2.0, and HT-HG-U133A), we selected genes common to all platforms based on the Entrez Gene ID and used the Median Rank Score method (20) for cross-platform normalization (Supplementary Fig. S1). Of 22,277 probes that were common among 3 Affymetrix platforms, 20,331 probes were selected to be in one to one relation between probe and gene. Using translation function based on Entrez Gene ID in GeneSpring GX 11.5, the 19,704 transcripts that matched to the 20,331 probes of the Affymetrix platform were extracted from all transcripts on the Agilent platform. Considering differences in microarray platforms, coefficient of correlation (r) in each gene between 2 microarray platforms were measured. Using 10 ovarian cancer microarray data obtained from both Agilent Whole Human Genome Oligo Microarray and Affymetrix HG-U133Plus2.0 (GSE32062), 9,141 genes with high correlation ($r > 0.8$) were extracted. After Median Rank Score analysis (20), we evaluated median value of each gene in both platforms and selected 3,553 genes with high correlation ($r > 0.8$) in which absolute value of subtracting median values between 2 platforms was less than 1. Similar analyses were conducted by 16 breast cancer microarray data (GSE17700; ref. 21) from both Affymetrix HG-U133Plus2.0 and HG-U133A. From the resulting 1,746 genes, we removed 60 that were not flagged as "Detected" in more than 90% of the Japanese data set A samples ($n = 260$), considering them to have either missing or uncertain expression signals. In addition, the data were normalized per gene in each data set by transforming the expression of each gene to obtain a mean of 0 and SD of 1 (Z-transformation) for the cross-platform study.

Published OnlineFirst January 12, 2012; DOI:10.1158/1078-0432.CCR-11-2725

We analyzed Japanese data set A as a "training set," Tothill's data set as a "test set," and the other 4 data sets as "validation sets." We applied elastic net analysis (22) with the R (23) package glmnet to identify survival-related genes for prediction of prognosis in patients with advanced stage high-grade serous ovarian cancer. Using 10-fold cross-validation, we obtained regression coefficients with optimal penalty parameter for the penalized Cox model, and calculated a prognostic index for each patient as defined by

$$\text{Prognostic index} = \sum_{i=1}^{126} \beta_i \times X_i$$

where $_i$ is the estimated regression coefficient of each gene in the Japanese data set A under elastic net ($\alpha = 0.05$) and X_i is the Z-transformed expression value of each gene. The estimated regression coefficient of each survival-related gene given by elastic net ($\alpha = 0.05$) in the Japanese data set A was also applied to calculate a prognostic index for each patient in 5 other data sets using the equation above. We classified all patients into the 2 groups (high- and low-risk groups) by the optimal cutoff value of the prognostic index in the Japanese data set A. Patients were assigned to the "high-risk" group if their prognostic index was more than or equal to cutoff value of prognostic index, whereas "low-risk" group was composed of cases with the prognostic indices that were less than cutoff value. Because risk classification divided by cutoff value 0.1517 indicated a minimum P value ($P = 1 \times 10^{-30}$) when log-rank test was used to compare differences in overall survival between high- and low-risk groups in the Japanese data set A, this value was determined as optimal cutoff value.

Both hierarchical clustering and non-negative factorization (NMF) algorithm (24) were used to assess the similarity of gene expression profiles among 126 survival-related genes. In the 2 major data sets (Japanese data set A and TCGA data set), we constructed a heat map with hierarchical clustering for both samples and genes using Cluster 3.0 (http://bonsai.hgc.jp/~mdehoon/software/cluster/software.htm). Correlation (centered) and complete linkage were selected on similarity metrics and clustering method, respectively. A heat map was visualized with Java TreeView (http://jtreeview.sourceforge.net/). NMF-consensus matrices averaging 50 connectivity matrices were computed at $K = 2$–7 (as the number of subclasses modeled) for 126 genes. With genes appearing along both the horizontal and vertical axes of the consensus matrices, consistency in the gene-pair clusters was visualized. We determined the optimal number of gene clusters by the cophenetic correlation coefficient that provides a scalar summary of global clustering robustness across the consensus matrix in the Japanese data set A and TCGA data set.

We conducted a volcano plot analysis to extract differentially expressed transcripts between high- and low-risk ovarian cancer groups with the 2 major data sets [Japanese data set A ($n = 260$) and TCGA data set ($n = 319$)]. When the volcano plot analysis was conducted in GeneSpring GX 11.5 (Agilent Technologies), we used gene expression data prior to Z-transformation normalization (Fig. 3).

To investigate the biological functions of gene expression signatures, we used GO Ontology Browser, embedded in GeneSpring GX11.5 (Agilent Technologies). The GO Ontology Browser was used to analyze which categories of gene ontology were statistically overrepresented among the gene list obtained. Statistical significance was determined by Fisher exact test, followed by multiple testing corrections by the Benjamini and Yekutieli false discovery rate method (25) To avoid bias of gene extraction by volcano plot analysis in GO analysis, Gene Set Enrichment Analysis (GSEA; ref. 26) was conducted with genes prior to gene selection by volcano plot analysis. Analysis settings in GSEA (software version 2.07) were as follows: (i) gene sets database: c5.all.v2.5.symbols.gmt [gene ontology], (ii) number of permutations: 1,000, (iii) collapse data set to gene symbol: true, (iv) permutation type: phenotype, (v) chip platform(s): Agilent_HumanGenome.chip or HT_HG_U133A.chip, and (vi) other settings: default.

Furthermore, we used the Core Analysis tool in the Ingenuity Pathway Analysis (IPA) system to analyze networks and pathways for a set of genes. Q value was calculated by Fisher exact test with the Benjamini and Hochberg correction (27). $Q < 0.25$ was considered as significant in GO, GSEA, and IPA.

Single-nucleotide polymorphism array experiments

We isolated genomic DNA from tumor tissues with a phenol-chloroform extraction method and from normal lymphocytes using the QIAamp DNA Blood Maxi Kit (QIAGEN). Single-nucleotide polymorphism (SNP) array experiments with the Genome-Wide Human SNP Array 6.0 (Affymetrix) were carried out at Niigata University (details in the Supplementary Methods). SNP array data were analyzed by the Partek Genomic Suite 6.5 (Partek Inc.) to investigate copy number variations in 30 genes involved in the antigen presentation pathway.

Immunoshitochemical analysis

A monoclonal anti-human CD8 antibody (M7103; 1:100; DAKO) was used for immunohistochemical staining of CD8 T lymphocyte in tumor tissues. Details of the immunohistochemistry method and sample selections are described in the Supplementary Methods.

Statistical analysis

Standard statistical tests including Pearson correlation analysis, unpaired t tests, 1-way ANOVA, Fisher exact tests, log-rank tests, and Cox proportional hazard model analysis were used to analyze the clinical data, as appropriate. Analyses of clinical data were conducted with JMP (version 8; SAS Institute) and GraphPad PRISM (version 4.0; GraphPad Software).

Published OnlineFirst January 12, 2012; DOI:10.1158/1078-0432.CCR-11-2725

Results

The distribution of the clinical variables for each microarray data set is shown in Table 1. To compare the microarray data sets measured with 4 different platforms, 1,686 genes were selected (Supplementary Fig. S1). An elastic net analysis (22) using 10-fold cross-validation on Japanese data set A (training set, $n = 260$) identified a 126-gene signature for predicting overall survival in patents with advanced stage high-grade serous ovarian cancer (Supplementary Table S1). After calculating the prognostic index for each sample from the 126-gene expression signature as reported previously (19), we divided the training set into high- and low-risk groups based on the optimal cutoff value (0.1517) of the prognostic index and verified the high predictive power of this risk classification (log-rank $P = 1 \times 10^{-30}$; Multivariate Cox $P = 4 \times 10^{-20}$; HR = 6.203; 95% CI = 4.239–9.123; Fig. 1A and Table 2).

The predictive power of the 126-gene signature was tested with Tothill's data set ($n = 131$; ref. 12). Both Kaplan–Meier survival and multivariate analysis showed that this risk classification was significantly associated with overall survival time in Tothill's data set (log-rank $P = 3 \times 10^{-6}$; Multivariate Cox $P = 1 \times 10^{-5}$; HR = 3.728; 95% CI = 2.110–6.532; Fig. 1B and Table 2). Next, we assessed the predictive power of the 126-gene expression signature on the 3 data sets in which microarray data were obtained from Affymetrix platforms and confirmed that this risk classification indicated similar results in the 3 data sets (Fig. 1C–E and Table 2). Furthermore, to exclude the influence of differences in microarray platforms, we prepared Japanese data set B from the same platform as the training set. Despite the small sample size, our risk classification showed a significant association with overall survival time in the Japanese data set B (Fig. 1F and Table 2). This risk classification showed high predictive accuracy even though

Table 1. Clinicopathologic characteristics in 6 microarray data sets

Data set	Japanese data set A	Tothill's data set[a]	Bonome's data set[a]	Dressman's data set[a]	TCGA data set[c]	Japanese data set B
Number	260	131	185	119	319	40
Age	58.2 ± 10.8	58.4 ± 9.8	62 ± 12	N/A[b]	59.5 ± 11.3	56.2 ± 9.6
Histology						
Serous	260	131	166	119	319	40
Others	0	0	19	0	0	0
Stage						
III	204	123	144	99	267	31
IV	56	8	41	20	52	9
Grade	Silverberg	Silverberg	N/A[b]	N/A[b]	N/A[b]	Silverberg
1	0	0	0	3	0	0
2	131	51	40	57	29	23
3	129	80	144	59	289	17
4	—	—	3	—	1	—
Surgery status						
Optimal	103	78	92	63	236	19
Suboptimal	157	45	93	56	83	21
Chemotherapy						
Platinum	260	131	185	119	319	40
Taxane	260	131	N/A	82	319	40
Follow-up period (mo)						
Median	42	29	38	34	31	39
Range	1–128	6–79	1–164	1–185	1–154	7–111
Number of deaths	121	60	129	69	187	22
Median survival (mo)	60	44	46	69	42	54
Microarray platform	Agilent Whole Human Genome Oligo Microarray	Affymetrix HG-U133 Plus2.0	Affymetrix HG-U133A	Affymetrix HG-U133A	Affymetix HT-HG-U133A	Agilent Whole Human Genome Oligo Microarray

[a]Clinical information in these 3 data sets were obtained from their articles and website.

[b]No available information was described as N/A.

[c]Publicly available clinical information in TCGA was downloaded from TCGA Data portal (http://tcga-data.nci.nih.gov/tcga/tcgaHome2.jsp) at June 25, 2011.

Published OnlineFirst January 12, 2012; DOI:10.1158/1078-0432.CCR-11-2725

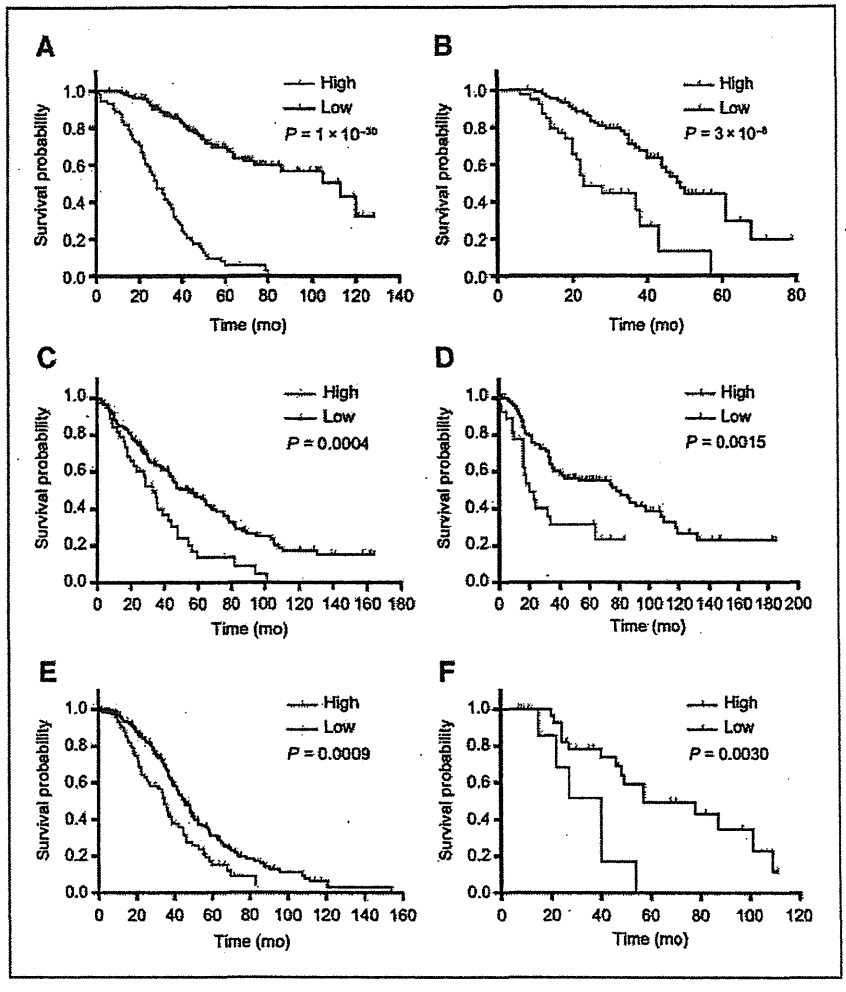

Figure 1. Kaplan–Meier survival analysis in 6 microarray data sets (A, Japanese data set A; B, Tothill's data set; C, Bonome's data set; D, Dressman's data set; E, TCGA data set; F, Japanese data set B). Based on 126-gene signature, ovarian cancer patients were divided into 2 risk groups (red, high risk; blue, low risk). *P* values correspond to the log-rank test comparing the survival curves.

overall survival was capped at 60 months (Supplementary Fig. S2; ref. 10). Moreover, the high-risk groups had shorter progression-free survival times compared with the low-risk groups in 4 microarray data sets with available progression-free survival times (Supplementary Fig. S3). In addition, we applied 193 overall survival related gene signature that have been recently reported by TCGA research networks (10) to our large data set (Japanese data set A), and 191 of 193 genes were available in our data set. High-risk ovarian cancer patients based on 191-gene signature model had significantly poor prognosis compared with low-risk patients (Supplementary Methods and Supplementary Fig. S4).

We next investigated the molecular characteristics of the 126-gene signature with both hierarchical clustering and NMF (24) analyses using the 2 major data sets (Japanese data set A and TCGA data set). Hierarchical clustering of the expression of 126 genes in the Japanese data set A ($n = 260$) resulted in 2 gene clusters (cluster 1 and 2; Fig. 2A). Cluster 1 (outlined in yellow in Fig. 2A) comprised 23 genes, 22 of which were common genes in a small cluster of NMF class assignment for $K = 2$ (Supplementary Fig. S5). Similarly, this gene cluster was seen both in hierarchical clustering and NMF analyses of TCGA data set, and the 20 genes in TCGA's cluster were consistent with these 23 genes in cluster 1 (Fig. 2B and Supplementary Fig. S5). GO analysis of these 23 genes revealed 132 significantly overrepresented GO categories; the top 20 GO categories are shown in the Supplementary Table S2. Specifically, immunity-related categories were enriched in these 23 genes and were downregulated in the high-risk groups compared with the low-risk groups. On the contrary, only 1 category [cytoplasm (GO0005737)] belonging to "cellular component" was significantly overrepresented in 103 genes of cluster 2.

To clarify the biological significance of our risk classification based on the 126-gene signature in advanced stage high-grade serous ovarian cancer, we examined differences in molecular biological characteristics between high- and low-risk groups. For subsequent analyses, all transcripts on

Published OnlineFirst January 12, 2012; DOI:10.1158/1078-0432.CCR-11-2725

Table 2. Univariate and multivariate Cox's proportional hazard model analysis of prognostic factors for overall survival

	Univariate analysis		Multivariate analysis	
	HR (95% CI)	*P*	HR (95% CI)	*P*
Japanese data set A				
Age	1.011 (0.993–1.029)	0.21	1.006 (0.988–1.024)	0.52
Stage IV (vs. stage III)	1.465 (0.968–2.165)	0.07	1.340 (0.884–1.984)	0.16
Optimal surgery (vs. suboptimal)	0.499 (0.334–0.730)	0.0003	0.643 (0.428–0.949)	0.026
High (vs. low)	6.823 (4.692–9.972)	2×10^{-22}	6.203 (4.239–9.123)	4×10^{-20}
Tothill's data set				
Age	1.005 (0.977–1.035)	0.73	1.006 (0.978–1.035)	0.67
Stage IV (vs. stage III)	2.264 (0.785–5.176)	0.12	2.951 (0.983–7.235)	0.053
Optimal surgery (vs. suboptimal)	0.887 (0.525–1.517)	0.66	0.910 (0.528–1.592)	0.74
High (vs. low)	3.443 (1.967–5.962)	3×10^{-5}	3.728 (2.110–6.532)	1×10^{-5}
Bonome's data set				
Optimal surgery (vs. suboptimal)	0.592 (0.414–0.840)	0.0032	0.628 (0.438–0.894)	0.0097
High (vs. low)	2.034 (1.341–3.012)	0.0011	1.897 (1.247–2.818)	0.0033
Dressman's data set				
Optimal surgery (vs. suboptimal)	0.685 (0.425–1.102)	0.12	0.602 (0.370–0.977)	0.04
High (vs. low)	2.397 (1.335–4.140)	0.0042	2.687 (1.480–4.705)	0.0016
TCGA data set				
Age	1.014 (1.001–1.028)	0.038	1.011 (0.997–1.025)	0.13
Stage IV (vs. stage III)	1.018 (0.683–1.469)	0.93	1.034 (0.692–1.499)	0.86
Optimal surgery (vs. suboptimal)	0.909 (0.668–1.254)	0.56	0.903 (0.654–1.261)	0.54
High (vs. low)	1.712 (1.234–2.345)	0.0015	1.680 (1.202–2.321)	0.0027
Japanese data set B				
Age	1.059 (1.007–1.118)	0.024	1.058 (0.999–1.131)	0.057
Stage IV (vs. stage III)	1.696 (0.542–4.501)	0.34	2.998 (0.808–10.60)	0.098
Optimal surgery (vs. suboptimal)	0.582 (0.231–1.364)	0.22	0.510 (0.175–1.413)	0.20
High (vs. low)	4.100 (1.376–11.25)	0.013	4.468 (1.265–15.49)	0.021

each platform were used to avoid the previous gene number limitations, which were for the cross-platform study. We extracted the genes differentially expressed between the 2 groups by carrying out a volcano plot analysis with the 2 major data sets (Japanese data set A and TCGA data set; Supplementary Table S3). Figure 3A shows that 1,109 and 1,381 transcripts were differentially expressed between the high- and low-risk groups in the Japanese data set A and TCGA data set, respectively. GO analysis of these transcripts indicated that 9 out of 20 top-ranked GO categories were common between both data sets and involved in the immune system (Table 3 and 4).

To exclude the influence of cutoff in fold change or *P* value in volcano plot analysis, we reevaluated differences in the biological characteristics between high- and low-risk groups using GSEA (26). Four immunity-related GO categories (immune system response, immune response, defense response, and inflammatory response) were also included in the list of 20 top-ranked GO categories when GSEA was carried out with 21,785 (Japanese data set A) and 14,023 (TCGA data set) transcripts prior to gene extraction (Supplementary Table S4).

Furthermore, possible functional relations among differentially expressed genes between high- and low-groups were investigated with pathway analysis. Of 20 top-ranked pathways notably enriched in 1,109 transcripts of the Japanese data set A and 1,381 transcripts of the TCGA data set, 14 pathways were common between both data sets (Supplementary Table S5). In particular, the antigen presentation pathway (Fig. 3B) was the most significantly overrepresented pathway in the 2 data sets (Japanese data set A, $Q = 2.0 \times 10^{-29}$; TCGA data set, $Q = 5.0 \times 10^{-14}$). In the antigen presentation pathway, 30 transcripts in this pathway were significantly downregulated in the high-risk group (Fig. 3B and Supplementary Table S6). We further examined whether molecular defects of human leukocyte antigen (HLA) class I antigen presentation machinery components were caused by structural alterations using SNP array data. Our SNP array data showed that genes of HLA class I antigen presentation machinery were not deleted (Supplementary Table S6). In the TCGA data set, only 10% of cases (24 of 242) had deletions in HLA class I genes. On the other hand, 89% of high-risk cases (55 of 62) without deletion in HLA class I genes showed significantly lower expressions in HLA class I genes compared with those in low-risk groups (Supplementary Fig. S6).

On the basis of this result, we assessed the status of tumor-infiltrating lymphocyte reflecting an immune response

Published OnlineFirst January 12, 2012; DOI:10.1158/1078-0432.CCR-11-2725

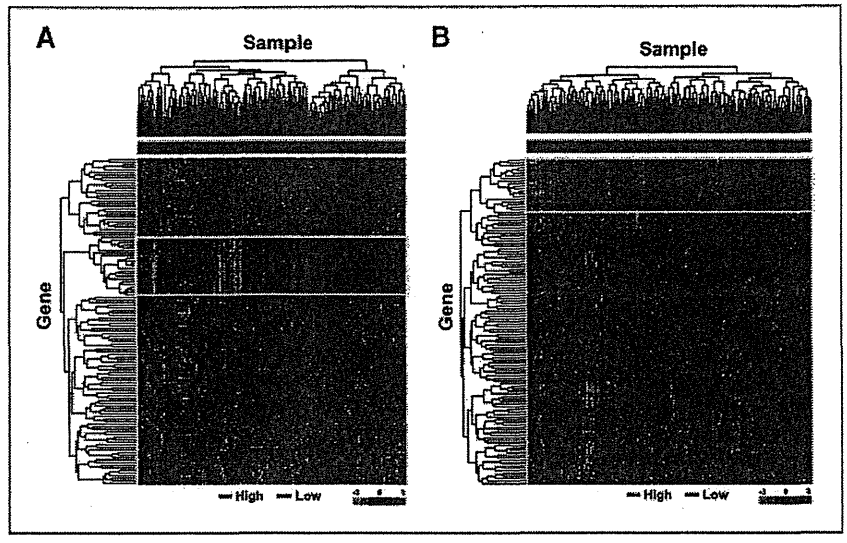

Figure 2. Molecular characteristics of 126 survival-related genes. A, heat map with a hierarchical classification of 260 patient samples with the expression profile of 126 survival-related genes in the Japanese data set A. B, heat map with a hierarchical classification of 319 patient samples with the expression profile of 126 survival-related genes in TCGA data set.

against ovarian cancer. By immunohistochemically staining for CD8-positive T lymphocytes in a subset of the Japanese data set ($n = 30$), we revealed that the number of CD8 T lymphocytes infiltrating into tumor tissues was significantly decreased in the high-risk group ($n = 10$) compared with the low-risk group ($n = 20$) and was clearly correlated with the expression level of HLA class I genes (Supplementary Fig. S7).

Table 3. Enriched GO categories among the transcripts significantly differentially expressed between high- and low-risk groups: top-ranked 20 of 534 significantly overrepresented categories ($Q < 0.25$) among 1,109 transcripts in Japanese data set A

	Genes within GO category		
GO category[a]	Number	Percentage	$-\text{Log}_{10}$ Q[b]
Immune system process (GO:0002376)	206	29.0	45.0
Immune response (GO:0006955)	172	24.2	45.0
Defense response (GO:0006952, 0002217, 0042829)	110	15.5	40.3
Response to stimulus (GO:0050896, 0051869)	251	35.4	29.2
Inflammatory response (GO:0006954)	68	9.6	26.2
Positive regulation of immune system process (GO:0002684)	40	5.6	25.2
Regulation of immune system process (GO:0002682)	52	7.3	24.5
Antigen processing and presentation (GO:0019882,0030333)	31	4.4	22.7
Signal transducer activity (GO:0004871, 0005062, 0009369, 0009370)	169	23.8	22.1
Molecular transducer activity (GO:0060089)	169	23.8	22.1
Signal transduction (GO:0007165)	224	31.5	20.8
Leukocyte activation (GO:0045321)	47	6.6	20.1
Cell activation (GO:0001775)	48	6.8	19.7
Regulation of immune response (GO:0050776)	32	4.5	18.9
Response to wounding (GO:0009611, 0002245)	70	9.9	18.7
Signal transmission (GO:0023060)	224	31.5	18.2
Signaling process (GO:0023046)	224	31.5	18.2
Regulation of cell activation (GO:0050865)	30	4.2	17.2
Positive regulation of cell activation (GO:0050867)	24	3.4	17.0
Regulation of lymphocyte activation (GO:0051249)	29	4.1	17.0

[a]Bold font denotes common categories included in top 20 lists both Japanese data set A and TCGA data set.
[b]Q value was determined by Fisher's exact test with Benjamini–Yekutieli correction.

Published OnlineFirst January 12, 2012; DOI:10.1158/1078-0432.CCR-11-2725

Table 4. Enriched GO categories among the transcripts significantly differentially expressed between high- and low-risk groups: top-ranked 20 of 83 significantly overrepresented GO categories ($Q < 0.25$) among 1,381 transcripts in TCGA data set

	Genes within GO category		
GO category[a]	Number	Percentage	$-\text{Log}_{10}\ Q$[b]
Immune system process (GO:0002376)	129	20.5	20.9
Immune response (GO:0006955)	115	18.3	20.8
Defense response (GO:0006952, 0002217, 0042829)	78	12.4	10.3
Antigen processing and presentation (GO:0019882, 0030333)	25	4.0	8.4
Inflammatory response (GO:0006954)	50	7.9	8.2
Antigen processing and presentation of peptide antigen (GO:0048002)	13	2.1	6.9
Antigen processing and presentation of exogenous peptide antigen (GO:0002478)	6	1.0	5.2
MHC class I peptide loading complex (GO:0042824)	9	1.4	5.2
MHC protein complex (GO:0042611)	18	2.9	5.2
TAP complex (GO:00042825)	8	1.3	5.2
MHC protein binding (GO:0042287)	12	1.9	5.2
Antigen processing and presentation of exogenous antigen (GO:0019884)	7	1.1	5.0
Response to stimulus (GO:0050896, 0051869)	183	29.1	4.4
Antigen processing and presentation of peptide antigen via MHC class I (GO:0002474)	7	1.1	3.9
Antigen processing and presentation of peptide or polysaccharide antigen via MHC class II (GO:0002504)	12	1.9	3.9
Regulation of immune response (GO:0050776)	6	1.0	3.8
MHC class I protein binding (GO:0042288)	10	1.6	3.8
Response to wounding (GO:0009611, 0002245)	50	7.9	3.8
Positive regulation of immune response (GO:0050778)	6	1.0	3.8
Positive regulation of immune system process (GO:0002684)	6	1.0	3.8

[a]Bold font denotes common categories included in top 20 lists both Japanese data set A and TCGA data set.
[b]Q value was determined by Fisher's exact test with Benjamini–Yekutieli correction.

Discussion

In this study, we established a novel risk classification system based on the 126-gene expression signature for predicting overall survival time in patients with advanced stage high-grade serous ovarian cancer. The significant association between our risk classification and overall survival time was indicated among the 6 microarray data sets.

In expression microarray analyses, there is a well-known "curse of dimensionality" problem that the number of genes is much larger than the number of samples. The curse of dimensionality leads to a concern about the reliability of the selected genes or an overfitting phenomenon, and using a large-scale microarray data is a simple and effective method to overcome this problem. From this theory, we planned a large-scale cross-platform study using 4 publicly available

Published OnlineFirst January 12, 2012; DOI:10.1158/1078-0432.CCR-11-2725

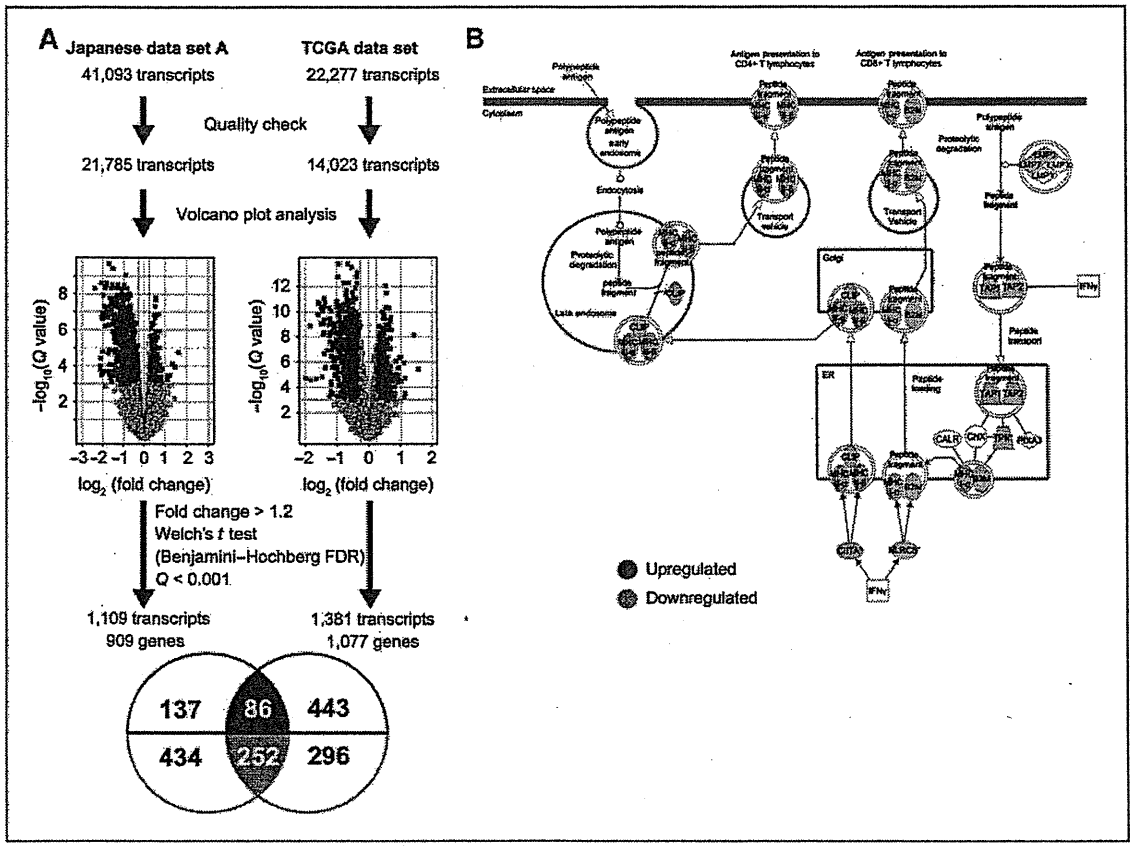

Figure 3. Molecular characteristics of differentially expressed genes between high- and low-risk groups in the 2 major data sets (Japanese data set A and TCGA data set). A, using a volcano plot analysis, 1,109 and 1,381 transcripts were extracted as differentially expressed genes between high- and low-risk groups in the Japanese data set A and TCGA data set, respectively. B, IPA showed that the antigen presentation pathway was significantly overrepresented in 1,109 Japanese data set A and 1,381 TCGA transcripts. Green indicates that gene expression was downregulated in high-risk group compared with low-risk group.

microarray data sets consisting of more than 100 samples. To carry out a cross-platform study, we took considerable care to reduce the influence of differences in microarray platforms with the Median Rank Score method and matching probes based on highly correlated expression ($r > 0.8$) between the 2 platforms. As a result, this risk classification system showed a high predictive ability in the 4 microarray data sets from different platforms. Our risk classification was suitably fitting to Japanese data set B despite the small sample size. This might reflect the same platform in the microarray experiments and similarity in clinical backgrounds between Japanese data set A and B. Intriguingly, 193 survival-related gene signature that has been reported by TCGA research networks (10) was also significantly associated with overall survival in our large data set (Supplementary Fig. S4), and 5 genes (*B4GALT5*, *CXCL9*, *ID4*, *MTRF1*, and *SLC7A11*) were common between their and our gene signatures despite different analytic processes (Supplementary Table 2). These genes might contribute strongly to developing risk classification system for high-grade serous ovarian cancer patients.

We ascertained that alterations to the immune system in cancer cells are one of the most important factors affecting survival of patients with advanced stage, high-grade serous ovarian cancer and that high-risk ovarian cancer was well characterized by the downregulation of the antigen presentation pathway at the molecular level.

The 2 large-scale subclassification studies (10, 11) based on gene expression analyses have indicated that there are at least 4 subclasses (immunoreactive, differentiated, proliferative, and mesenchymal) in high-grade serous ovarian cancer. Although there was no statistically significant difference in clinical outcome among 4 subclasses, this finding that immunity-related genes are identified in large-scale gene expression profiles despite different analytic approaches suggests that alteration of immune activity might play an important role in the molecular characterization of ovarian cancer.

Published OnlineFirst January 12, 2012; DOI:10.1158/1078-0432.CCR-11-2725

Previous findings (28–30) that the presence of tumor-infiltrating T lymphocytes is associated with long survival in ovarian cancer patients are consistent with the results from our comprehensive gene expression analysis using large-scale microarray data, suggests that the presence of immune responses to cancer cells would influence the biological phenotype of ovarian cancer. Although several antigen-specific active immunotherapy studies have been conducted, the clinical benefit of this approach has not yet been shown in large randomized-controlled trials (31, 32). Previous reports (28, 33, 34) and our data indicated that defects in HLA class I antigen presentation machinery would decrease recruitment of tumor-infiltrating lymphocytes, leading to poor prognosis in cancer patients because of a reduction in antitumor immune activity. Therefore, upregulation of HLA class I antigen presentation pathway might be one of efficient therapeutic approach for patients with high-risk serous ovarian cancer, especially when antigen-specific active immunotherapy is selected as a therapeutic strategy (35).

Defects of HLA class I gene expression occurs at the genetic, epigenetic, transcriptional, and posttranscriptional levels, and are classified into the 2 main groups: reversible and irreversible defects (36). Our data show that the frequency of deletion leading to irreversible defect of HLA class I gene expression was low in high-grade serous ovarian cancer. Only a few HLA class I gene mutations have been described thus far (36). Downregulation of antigen presentation machinery components such as *TAP1/2* or *B2M* also result in reversible defects in HLA class I molecules (37). Interestingly, the expression levels of genes in the antigen presentation pathway were positively correlated in the Japanese data set A (Supplementary Fig. S8). IFN-γ or other cytokines stimulation induces the expression of genes in the antigen presentation pathway (38). Moreover, histone deacetylase (HDAC) inhibitors increase the expression of genes in the antigen presentation pathway such as *TAP1/2* (39, 40) and *B2M* (41) in several cancer cells leading to upregulating the antigen presentation pathway. In addition, HDAC inhibitors that are promising anticancer drugs show a synergistic effect with taxane or platinum drugs, which were used as standard adjuvant chemotherapy for ovarian cancer, both *in vitro* and *in vivo* (42, 43). These genetic and epigenetic activations of the antigen presentation pathway might induce immune recognition of ovarian cancer cells and enhance antitumor immune responses.

In summary, our data suggest that this predictive biomarker based on the 126-gene signature could identify patients who should not expect long-term survival by standard treatment and that activation of the antigen presentation pathway in tumor cells is an important key in new therapeutic strategies for ovarian cancer.

Disclosure of Potential Conflicts of Interest

No potential conflicts of interest were disclosed.

Acknowledgments

The authors thank Prof. Y. Nakamura for his help, the tissue donors and supporting medical staff for making this study possible, C. Seki and A. Yukawa for their technical assistance, T. Mizuochi for discussion, Prof. S. G. Silverberg for his enthusiastic help with the pathologic review, and K. Boroevich for helpful comments on the manuscript.

The costs of publication of this article were defrayed in part by the payment of page charges. This article must therefore be hereby marked *advertisement* in accordance with 18 U.S.C. Section 1734 solely to indicate this fact.

Received October 24, 2011; revised December 9, 2011; accepted December 23, 2011; published OnlineFirst January 12, 2012.

References

1. Cannistra SA. Cancer of the ovary. N Engl J Med 2004;351:2519–29.
2. Kurman RJ, Visvanathan K, Roden R, Wu TC, Shih Ie M. Early detection and treatment of ovarian cancer: shifting from early stage to minimal volume of disease based on a new model of carcinogenesis. Am J Obstet Gynecol 2008;198:351–6.
3. Levanon K, Crum C, Drapkin R. New insights into the pathogenesis of serous ovarian cancer and its clinical impact. J Clin Oncol 2008;26:5284–93.
4. Bowtell DD. The genesis and evolution of high-grade serous ovarian cancer. Nat Rev Cancer 2010;10:803–8.
5. Winter WE 3rd, Maxwell GL, Tian C, Carlson JW, Ozols RF, Rose PG, et al. Prognostic factors for stage III epithelial ovarian cancer: a Gynecologic Oncology Group Study. J Clin Oncol 2007;25:3621–7.
6. du Bois A, Reuss A, Pujade-Lauraine E, Harter P, Ray-Coquard I, Pfisterer J. Role of surgical outcome as prognostic factor in advanced epithelial ovarian cancer: a combined exploratory analysis of 3 prospectively randomized phase 3 multicenter trials: by the Arbeitsgemeinschaft Gynaekologische Onkologie Studiengruppe Ovarialkarzinom (AGO-OVAR) and the Groupe d'Investigateurs Nationaux Pour les Etudes des Cancers de l'Ovaire (GINECO). Cancer 2009;115:1234–44.
7. Dowsett M, Dunbier AK. Emerging biomarkers and new understanding of traditional markers in personalized therapy for breast cancer. Clin Cancer Res 2008;14:8019–26.
8. Weigelt B, Baehner FL, Reis-Filho JS. The contribution of gene expression profiling to breast cancer classification, prognostication and prediction: a retrospective of the last decade. J Pathol 2010;220:263–80.
9. Ahmed AA, Etemadmoghadam D, Temple J, Lynch AG, Riad M, Sharma R, et al. Driver mutations in TP53 are ubiquitous in high grade serous carcinoma of the ovary. J Pathol 2010;221:49–56.
10. The Cancer Genome Atlas Research Network. Integrated genomic analyses of ovarian carcinoma. Nature 2011;474:609–15.
11. Tothill RW, Tinker AV, George J, Brown R, Fox SB, Lade S, et al. Novel molecular subtypes of serous and endometrioid ovarian cancer linked to clinical outcome. Clin Cancer Res 2008;14:5198–208.
12. Bonome T, Levine DA, Shih J, Randonovich M, Pise-Masison CA, Bogomolniy F, et al. A gene signature predicting for survival in suboptimally debulked patients with ovarian cancer. Cancer Res 2008;68:5478–86.
13. Dressman HK, Berchuck A, Chan G, Zhai J, Bild A, Sayer R, et al. An integrated genomic-based approach to individualized treatment of patients with advanced-stage ovarian cancer. J Clin Oncol 2007;25:517–25.
14. Majewski IJ, Bernards R. Taming the dragon: genomic biomarkers to individualize the treatment of cancer. Nat Med 2011;17:304–12.
15. Heintz AP, Odicino F, Maisonneuve P, Beller U, Benedet JL, Creasman WT, et al. Carcinoma of the ovary. J Epidemiol Biostat 2001;6:107–38.
16. Eisenhauer EA, Therasse P, Bogaerts J, Schwartz LH, Sargent D, Ford R, et al.: New response evaluation criteria in solid tumours: Revised RECIST guideline (version 1.1). Eur J Cancer 2009;45:228–47.

Published OnlineFirst January 12, 2012; DOI:10.1158/1078-0432.CCR-11-2725

17. Tavassoli FA, Devilee P. World Health Organization Classification of Tumors. Pathology & Genetics. Tumors of the breast and female genital organs. Lyon (France): IARC Press; 2003. p. 117–45.
18. Silverberg SG. Histopathologic grading of ovarian carcinoma: a review and proposal. Int J Gynecol Pathol 2000;19:7–15.
19. Yoshihara K, Tajima A, Yahata T, Kodama S, Fujiwara H, Suzuki M, et al. Gene expression profile for predicting survival in advanced-stage serous ovarian cancer across two independent datasets. PLoS One 2010;5:e9615.
20. Glaab E, Garibaldi J, Krasnogor N. ArrayMining: a modular web-application for microarray analysis combining ensemble and consensus methods with cross-study normalization. BMC Bioinformatics 2009;10:358.
21. Symmans WF, Hatzis C, Sotiriou C, Andre F, Peintinger F, Regitnig P, et al. Genomic index of sensitivity to endocrine therapy for breast cancer. J Clin Oncol 2010;28:4111–9.
22. Simon N, Friedman J, Hastie T. Regularization paths for Cox's proportional hazards model via coordinate descent. J Stat Softw 2010;39:1–22.
23. R Development Core Team. R: A language and environment for statistical computing. 2011
24. Brunet JP, Tamayo P, Golub TR, Mesirov JP. Metagenes and molecular pattern discovery using matrix factorization. Proc Natl Acad Sci U S A 2004;101:4164–9.
25. Benjamini Y, Yekutieli D. The control of the false discovery rate in multiple testing under dependency. Ann Stat 2001;29:1165–88.
26. Subramanian A, Tamayo P, Mootha VK, Mukherjee S, Ebert BL, Gillette MA, et al. Gene set enrichment analysis: A knowledge-based approach for interpreting genome-wide expression profiles. Proc Natl Acad Sci U S A 2005;102:15545–50.
27. Benjamini Y, Hochberg Y. Controlling the false discovery rate: a practical and powerful approach to multiple testing. J R Statist Soc B 1995;57:289–300.
28. Han LY, Fletcher MS, Urbauer DL, Mueller P, Landen CN, Kamat AA, et al. HLA class I antigen processing machinery component expression and intratumoral T-Cell infiltrate as independent prognostic markers in ovarian carcinoma. Clin Cancer Res 2008;14:3372–9.
29. Leffers N, Fehrmann RS, Gooden MJ, Schulze UR, Ten Hoor KA, Hollema H, et al. Identification of genes and pathways associated with cytotoxic T lymphocyte infiltration of serous ovarian cancer. Br J Cancer 2010;103:685–92.
30. Gooden MJ, de Bock GH, Leffers N, Daemen T, Nijman HW. The prognostic influence of tumour-infiltrating lymphocytes in cancer: a systematic review with meta-analysis. Br J Cancer 2011;105:93–103.
31. Leffers N, Daemen T, Helfrich W, Boezen HM, Cohlen BJ, Melief K, et al. Antigen-specific active immunotherapy for ovarian cancer. Cochrane Database Syst Rev 2010;1:CD007287.
32. Kandalaft LE, Powell DJ Jr, Singh N, Coukos G. Immunotherapy for ovarian cancer: what's next? J Clin Oncol 2011;29:925–33.
33. Rolland P, Deen S, Scott I, Durrant L, Spendlove I. Human leukocyte antigen class I antigen expression is an independent prognostic factor in ovarian cancer. Clin Cancer Res 2007;13:3591–6.
34. Shehata M, Mukherjee A, Deen S, Al-Attar A, Durrant LG, Chan S. Human leukocyte antigen class I expression is an independent prognostic factor in advanced ovarian cancer resistant to first-line platinum chemotherapy. Br J Cancer 2009;101:1321–8.
35. Tanaka K, Hayashi H, Hamada C, Khoury G, Jay G. Expression of major histocompatibility complex class I antigens as a strategy for the potentiation of immune recognition of tumor cells. Proc Natl Acad Sci U S A 1986;83:8723–7.
36. Garrido F, Cabrera T, Aptsiauri N. "Hard" and "soft" lesions underlying the HLA class I alterations in cancer cells: implications for immunotherapy. Int J Cancer 2010;127:249–56.
37. Khong HT, Restifo NP. Natural selection of tumor variants in the generation of "tumor escape" phenotypes. Nat Immunol 2002;3:999–1005.
38. Dunn GP, Koebel CM, Schreiber RD. Interferons, immunity and cancer immunoediting. Nat Rev Immunol 2006;6:836–48.
39. Khan AN, Gregorie CJ, Tomasi TB. Histone deacetylase inhibitors induce TAP, LMP, Tapasin genes and MHC class I antigen presentation by melanoma cells. Cancer Immunol Immunother 2008;57:647–54.
40. Setiadi AF, Omilusik K, David MD, Seipp RP, Hartikainen J, Gopaul R, et al. Epigenetic enhancement of antigen processing and presentation promotes immune recognition of tumors. Cancer Res 2008;68:9601–7.
41. Kitamura H, Torigoe T, Asanuma H, Honma I, Sato N, Tsukamoto T. Down-regulation of HLA class I antigens in prostate cancer tissues and up-regulation by histone deacetylase inhibition. J Urol 2007;178:692–6.
42. Chobanian NH, Greenberg VL, Gass JM, Desimone CP, Van Nagell JR, Zimmer SG. Histone deacetylase inhibitors enhance paclitaxel-induced cell death in ovarian cancer cell lines independent of p53 status. Anticancer Res 2004;24:539–45.
43. Qian X, LaRochelle WJ, Ara G, Wu F, Petersen KD, Thougaard A, et al. Activity of PXD101, a histone deacetylase inhibitor, in preclinical ovarian cancer studies. Mol Cancer Ther 2006;5:2086–95.

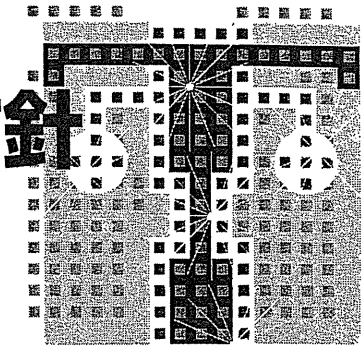

早期卵巣がんの治療方針

大亀真一
国立病院機構四国がんセンター婦人科
野河孝充
国立病院機構四国がんセンター手術部長

卵巣は腹腔内に直接露出する形で存在するため，卵巣腫瘍の表面にがんが出てくると急速に腹腔内全体に広がります。卵巣がんの多くは無症状で経過し，腫瘍の増大にともなって腹部にしこりを触れることや，多量の腹水による腹部膨満感などの症状が出現した進行がんで発見されます。このため卵巣がんはサイレントキラーと呼ばれることもあり，早期がんでの発見が困難とされています。

卵巣がんの5年生存率（表1）は，がんが卵巣に限局するⅠ期や骨盤内にとどまるⅡ期は90～70%，骨盤外に広がるⅢ期や肺などへ転移したⅣ期では40～30%と，進行がんでは極端に悪くなります。卵巣がんの治療は手術で可能なかぎりがんを摘出し，化学療法（抗がん剤投与）を併用する方法が基本的な治療法になります。

卵巣がんではⅠ～Ⅱ期が早期とされますが，Ⅱ期は進行がんと同じように，手術後に化学療法が必要となります。本稿では，卵巣に限局してがんが存在する場合，つまり進行期ではⅠ期にあたる卵巣がんを「早期卵巣がん」と定義して，その治療方針について説明します。

手術前の診断

さまざまな検査方法により「卵巣がんⅠ期です」と診断された場合，がんは卵巣に限局している可能性が高いということを意味しています。お腹の中にがんが散らばっている状態（腹腔内播種，進行期Ⅱ～Ⅲ期）や肺や肝臓などへの転移（遠隔転移，進行期Ⅳ期）を明らかに認めない状態です。しかし，検査によるⅠ期という診断は予測にしかすぎません。治療方法の決定には，正確な進行期とがんの組織型を確定することが必要です。診断の確定は，手術で摘出した臓器を，顕微鏡で観察する検査（病理診断）によって行われます。

表1　卵巣がんの5年生存率（%）

進行期	5年生存率
Ⅰ期	90.30
Ⅱ期	76.30
Ⅲ期	42.40
Ⅳ期	32.60

〔文献1より引用〕

手術療法

卵巣がんに対する基本手術術式（staging laparotomy；進行期を確定するために必要な手術）は，両側卵巣卵管摘出術，子宮全摘術，大網切除術，後腹膜リンパ節郭清術，腹膜生検および腹腔細胞診から構成されています。

がんが存在する部位（原発部位）が片側であっても左右卵巣卵管を摘出すること，卵巣と密接な関係にある子宮を摘出すること，卵巣がんが転移しやすい臓器である大網を切除すること，卵巣から他部位への転移経路の一つであるリンパ節を切除すること，転移が疑わしい部位（腹膜など）の切除，肉眼的にはわからないがん細胞が存在している可能性のある腹水や腹腔内を洗浄した生理食塩水などを検査することが，進行期を決定するために必要とされています。

この基本手術を施行し，摘出してきた卵巣以外の臓器にがん組織が存在しているかどうかで，Ⅰ期なのかあるいはⅡ～Ⅲ期なのかという診断を下します。つまり，がんを取り除くという「治療」と，他部位におけるがんの有無を調べるという「検査」とを兼ね備えた手術と考えることができます。

リンパ節転移がないⅠ期卵巣がんと考えられた症例の約15％において，病理診断によってリンパ節転移が発見されています。このように早期卵巣がんと予測している場合でも，この基本手術を行い，正確な進行期を決定することが，その後の適切な治療を行う際に必須となります。

ただし，リンパ節郭清は手術領域が広範囲に及び，術中出血量の増加や手術時間の延長，下肢リンパ浮腫やリンパ膿瘍といった術後合併症がおこる可能性があります。このような身体への負担が大きい手術を受けるときの年齢や全身状態は，リンパ節すべてを切除する「郭清」とするか，疑わしいリンパ節を選択切除する「生検」とするかなど，手術範囲の決定に重要な要素となります。担当医には，過去から現在までの病歴や使用している薬剤を正確に伝え，どのような手術方法が適しているかということの説明を受けてください。

病理組織診断

手術で摘出された臓器は，顕微鏡を用いて観察する検査を経て，確定診断（病理診断）がつけられます。大きく分けて，進行期，組織型および組織学的分化度の診断がつくことになります。

進行期Ⅰ期は，がんが片側卵巣に限局しているⅠa期，がんが両側卵巣に限局しているⅠb期，がんは卵巣に限局しているが，卵巣表面までがんが浸潤（被膜表面への浸潤）していたり，卵巣が破れていたり（被膜破綻），腹水にがん細胞を認めたりするⅠc期に分類されます。

おもな組織型として，卵巣表面を被う膜から発生する表層上皮性腫瘍の漿液性腺癌，粘液性腺癌，類内膜腺癌，明細胞腺癌があげられます。明細胞腺癌以外の三つの組織型に関しては，同じ組織型でも悪性度の違いがあり，組織学的分化度という診断も同時に行われます。その分類では，高分化型（grade 1），中分化型（grade 2），低分化型（grade 3）の順に悪性度が高くなります。

これらの進行期，組織型，組織学的分化度に応じて，手術後の治療方針が決定されます。

手術後の治療方針

図１を参照してください。卵巣がんの診療において，現時点で適正とされる治療方針を示した『卵巣がん治療ガイドライン　2010年版』に掲載している表を改変したものです。

進行期Ⅰa期，Ⅰb期で，組織型は明細胞腺癌以外，組織学的分化度は高分化型である場合には，手術後は外来での経過観察となります。

進行期Ⅰa，Ⅰb期でも，組織型が明細胞腺癌である場合，組織型は明細胞腺癌以外だが組織学的分化度が中～低分化型である場合，進行期がⅠc期である場合は，術後治療とし

図1　治療フローチャート（Ⅰ期卵巣がん）

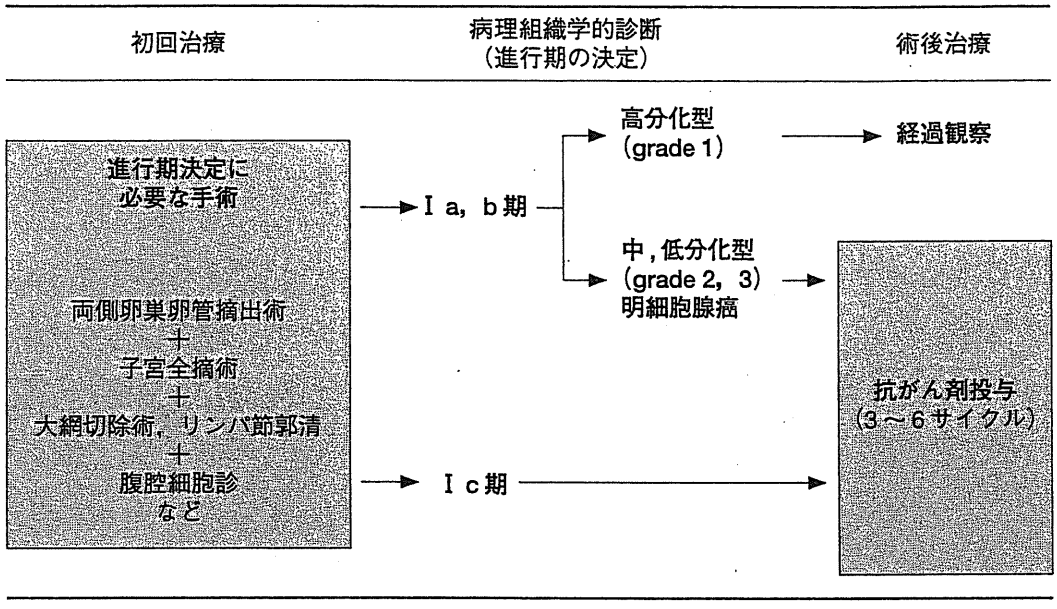

〔文献2より引用，一部改変〕

て抗がん剤による治療（化学療法）が必要となります。

卵巣がん手術後の化学療法は，パクリタキセルとカルボプラチンの2剤を3～4週ごとに3～6サイクル併用投与する方法（TC療法）が標準的治療とされています。パクリタキセルを週ごとに分割投与する方法も，最近有効性が確認されています。

抗がん剤投与によってもたらされる副作用が強い場合や，手術で確認された組織型によっては，異なった抗がん剤を選択することもあります。

＊

卵巣がんを早期に発見するための確立された検診方法はありません。しかし，経腟超音波検査では，卵巣が腫大していることを容易に発見できます。子宮がん検診を定期的に受診し，その際に超音波検査で卵巣を確認することも必要であると考えます。

卵巣がんⅠ期の5年生存率は90%以上で，比較的予後良好な疾患とされています。しかし，少ないながらも数%認められる再発を早期に発見するためには，初回治療後も定期的な検診を受けることが必要となってきます。

〈参考文献〉
1）日本産科婦人科学会婦人科腫瘍委員会：婦人科腫瘍委員会報告 第51回治療年報（卵巣悪性腫瘍）．日産婦誌 64：1117-1133，2012
2）日本婦人科腫瘍学会編：卵巣がん治療ガイドライン　2010年版．金原出版，2010

［おおかめ・しんいち／婦人科］
［のがわ・たかよし／婦人科］

婦人科腫瘍登録

－本邦の婦人科腫瘍登録と頸癌・体癌取扱い規約の改訂について－

四国がんセンター手術部長　野　河　孝　充

周知のように日本産科婦人科学会の婦人科腫瘍委員会により，当初は子宮頸癌に始まり，ついで体癌，卵巣癌の全国的な登録と予後調査集計事業がおこなわれ，各腫瘍の患者年報と治療年報がannual reportとして報告されている。例年，6月30日は日産婦婦人科腫瘍委員会への新規患者の登録と3年，5年予後追跡調査の報告の締切日である。四国がんセンターでは年明けから6月の締め切りにあわせて，各腫瘍に対するデータベースの作成と予後調査を行っている。近年，体癌，卵巣癌患者の増加，治療法の多様化に伴いデータベース作成に長時間の労力を要し，登録に必要な項目のみの先行集計になる場合もある。また，予後調査は治療成績をみるために最も重要な事項であるが，愛媛県を主体とする患者移動の少ない地域の調査であっても10％弱の追跡不能症例がでるのが課題となる。婦人科腫瘍委員会の2010年度患者年報をみると，現在，この腫瘍登録事業に301機関が参加している。Ⅰ～Ⅳ期の各癌種の登録数をみると，子宮頸癌が6,582例，体癌が6,665例，卵巣癌が4,356例，卵巣境界悪関腫瘍は1,348例である。全国レベルでみると，婦人科の主要な癌種である子宮頸癌，体癌，卵巣癌の本邦での罹患数は，卵巣癌が若干少ないもののほぼ同数となる。また登録方法は，永年にわたり紙ベースの登録用紙で行われてきたが，コンピュターの普及に伴い平成10年フロッピーディスク用いた登録法に変わり，平成15年度より，個人情報保護のもとに，連結不可能匿名化して，インターネット登録になっている。

日産婦学会員は周知のように，2008年に子宮頸癌，体癌と外陰癌のFIGO進行期分類改定が行われ，また子宮肉腫の進行期分類が新たに設定された。婦人科腫瘍委員会も取扱い規約を改定し，2012年症例から新進行期による登録作業となる。

現在，登録がおこなわれている子宮頸癌と体癌についての改定をみると，子宮頸癌は従来と同じく臨床進行期分類が採用され，主な変更事項について，ⅡA期は腫瘍径が予後に影響することから，4cm径でⅡA1とⅡA2期に細分類されたことで大きな変化はない。子宮体癌は従来の手術進行期を用いるが，頸癌に比べて改訂項目が多数となった。主な改定は，旧ⅠA期とⅠB期の予後に差が無いことから，筋層浸潤1/2未満は1A期，旧1C期は1B期になった。頸部浸潤のあるⅡ期については，間質浸潤のあるもののみがⅡ期とされ，旧2A期は1期に分類された。腹水（洗浄）細胞診は独立した危険因子ではないとされ分類から除外された。リンパ節転移に関しては骨盤リンパ節転移と傍大動脈リンパ節転移を区別し，骨盤リンパ節のみ転移はⅢC1期，傍大動脈リンパ節転移があるとⅢC2期の分類になった。今回の改訂で特筆すべき点は，従来，CTやMRIの画像検査所見は進行期決定に反映されなかったが，画像診

断を腫瘍の進展度合いや腫瘍サイズの評価に用いても構わないとされた点である。本邦では，悪性腫瘍の治療前検査にはCT，MRI，PETによる画像診断がほぼ全例におこなわれており，より正確な進行期の決定と予後への反映が期待される。

婦人科腫瘍委員会の登録実施要項をみると，主な登録項目は患者No（自動表示），年齢，進行期分類の選択（臨床進行期，手術進行期，NAC例），FIGO進行期，TNM分類，pTNM（子宮頸癌），組織型，治療開始年月日，治療法を入力していくのは従来と同じである。今回，画像診断の採用のため，子宮頸癌は腫瘍サイズ，基靭帯浸潤，膀胱浸潤，骨盤と傍大動脈およびその他のリンパ節腫大有無，遠隔転移有無の項目が新たに追加された。体癌も非手術例における筋層浸潤とリンパ節転移有無を，CT，MRI，PETなどの検査法も含めて入力することになり，病態の把握が詳細になるも，入力作業の煩雑化が予想される。放射線専門医の不在施設では，婦人科医自身の画像診断能力のレベルアップが要求される。また，リンパ節腫大に関しては従来と同じく，手術時触診，画像検査共にサイズの明確な規定が無く診察医の主観的な判定になる。

登録された症例データーは各委員にまわされ，症例ごとの登録内容のチェックを受けて患者年報となる。四国がんセンター日浦昌道元手術部長も腫瘍委員として，一連の業務の関わり内容を垣間見る機会があった。進行期の表記は一見簡単なようであるが，取扱い規約の読み込みと習熟が必要で，施設間の腫瘍登録に対する重要性の認識の違いには興味深い点が多々みられた。腫瘍委員会も登録作業の疑問点に随時回答できる体制を整備し，腫瘍登録の精度管理の重要性を周知していくことが必要である。

治療年報は3年と5年予後を報告する。カルテ上で5年予後が判るのは，受診患者の多くが愛媛県に在住し，治療後も引き続き通院する四国がんセンター婦人科においても，良くて70～80%である。婦人科腫瘍委員会の予後報告から登録施設間の追跡率を比較していくと，登録患者数の多い上位の施設ほど予後調査の充実が一目瞭然であるが，なかには事情によるのか腫瘍専門の施設でも追跡率不良があり興味が湧く。腫瘍委員会は，第49回治療年報から，予後解析の精度を上げるために，追跡不能症例が20%を超える施設のデーターは治療成績の解析に不採用とした。

また，生存率の解析方法は従来の直接法最小生存率による方法（消息不明例を死亡とみなすか生存とみなすか，また除外して計算するかで3種類の生存率がでる）からKaplan－Meier法に変更した。2001年治療年報から，解析対象数は減少したが生存率の精度が改善されたことになる。

平成19年の癌対策基本法の施行後，がん治療の均てん化が言われ，また院内がん登録，地域がん登録事業も推進されてきたが，最も必要な精度の高い全国レベルの予後調査の取り組みは遅れているのが実情である。非来院患者の追跡調査の方法は転院先病院への照会，患者への郵便や電話による個別の問い合わせがあるが，転居や固定電話の解約などでかなりの追跡不能者がでる。最終的には市町村自治体への照会となるが，個人情報保護法を理由に非協力や住民票照会料金の請求もあり，さらに死因の把握には死亡診断書の内容照会も必要であり，広く国民の理解と行政に対する要請が課題である。

2. ヒステロスコピーのコツ

1)ヒステロスコピーとは(図81)

- 子宮腔内を直視下と同様に観察できるため，病巣の形態，部位，広がり，単発性か多発性か，良・悪性の判定，特に小病変の診断に有用である．
- ヒステロスコープには直線的な硬性鏡と，先端部が前後に屈曲して視野角度が広く，操作性に優れた軟性鏡がある．
- 軟性鏡にはファイバースコープ(先端部外径3.0mm)と，電子スコープ(先端部外径3.8mm)があり，後者は先端部に超小型のCCDを搭載しており，より画像が鮮明である．
- 両者とも頸管拡張することなく子宮腔へ挿入でき，外来での検査に適している．
- 本項では，診断用の軟性ヒステロスコープによる検査について述べる．

2)適応と注意(表20)

〈適応〉 臨床的に子宮体癌を疑うが，組織診断に至らないものが対象となる．

〈注意〉 子宮腔内への機器挿入と灌流液注入の影響を考慮する．

ヒステロスコピーを行うことにより腹腔内へ癌細胞を流出させるという明確な根拠はない．また生命予後との関連もない．

術前に表20の疾患の有無を確認する．

3)説明と同意

- ヒステロスコピーの目的，検査方法，合併症や検査の限界などを十分に説明し，必ず同意を得る．

4)合併症

- 診断用ヒステロスコープは外径が細く，挿入が容易で侵襲も少なく，合併症はまれである．
- 合併症には感染症，病巣からの接触出血，子宮壁穿孔，頸管裂傷がある．
- 空気や炭酸ガスによる子宮腔拡張では塞栓がある．

●全身的なものでは迷走神経反射によるショックなどがある.

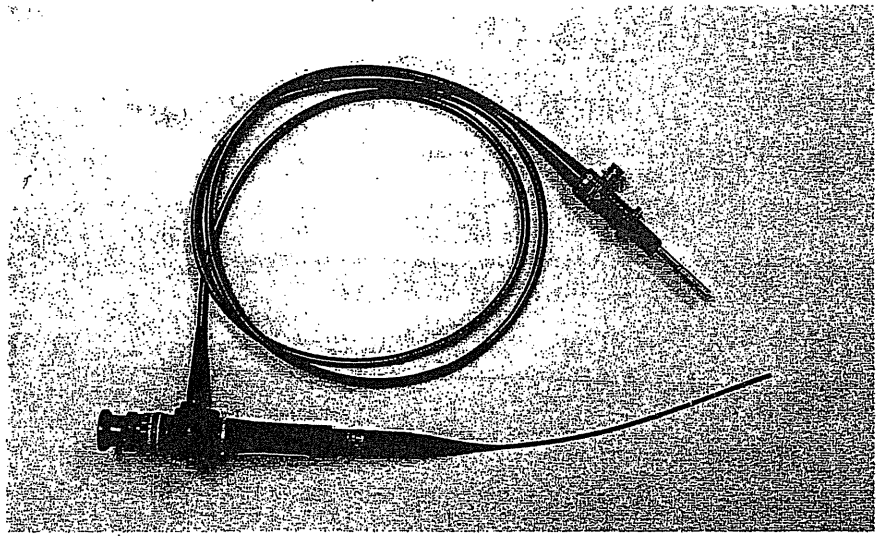

図81. ヒステロファイバースコープ

表20. ヒステロスコピーの適応と禁忌

1. 適応…子宮体癌が疑われる ①不正性器出血：月経異常，更年期出血，閉経後出血 ②掻爬診で確定診断不能な内膜細胞診異常 ③子宮頸部細胞診の異型腺細胞(AGC) ④子宮体癌の存在が疑われる組織診異常(子宮内膜増殖症) ⑤超音波，CT，MRI，PET-CT 検査などの子宮内膜異常所見 (異常内膜肥厚；閉経前＞20 mm，閉経後＞5 mm) ⑥過多月経，月経困難症 ⑦原因不明の不妊症
2. 禁忌 ①性器(腟，子宮，卵管)，骨盤内に感染症があるとき ②妊娠，もしくは妊娠の可能性があるとき ③子宮鏡検査で出血の増量が予想される場合
3. 禁忌でないが注意を要する 狭心症，不整脈などの心疾患，脳動脈瘤，抗凝固薬服用，出血傾向の患者

5)検査手順—診断用軟性ヒステロスコープ(図82)

①検査の時期は，閉経前では月経終了後の内膜肥厚のない増殖期の初期が適している．出血があるときは，出血の減少や止血を待って検査を行う．

②子宮鏡の洗浄と消毒は，各機器の説明書に従うが，ガス(EOG)滅菌が望ましい．

③子宮腔拡張には，子宮内浮遊物や血液を洗い出せる灌流液が有用である．生理食塩水，ブドウ糖液やデキストランを，50～70cmの高さから自然落差で灌流させる．

④通常，鎮痛薬投与と麻酔は不要である．

⑤双合診で子宮の位置，方向，大きさを確認する．

⑥ヒステロスコープの挿入前に，超音波断層法で子宮頸管から内腔の走行を確認する．

⑦頸管拡張と子宮ゾンデ探査も不要であるが，挿入は内子宮口までに留める．過度の頸管拡張は灌流液が子宮外へ流出しやすくなり，子宮腔が加圧不足となり観察に支障をきたす．

⑧灌流液を流しながら，頸管内の病変の有無，性状を観察しつつヒステロスコープを挿入していく．単鉤膣部鉗子で子宮を牽引把持すると，容易に挿入でき観察しやすい．

⑨子宮体癌では頸管浸潤の有無を確認する．

⑩先端部が内子宮口を超えたら挿入を止めて子宮腔の拡張を待つ．血液や浮遊物による子宮内の混濁に対しては，ヒステロスコープを引き戻して混濁液の子宮外流出を繰り返し，鮮明化を待つ．

⑪まず両側卵管口を含む子宮腔全体を観察し，病変の有無，部位，形態，広がり，個数を確認する．とくに小病変を見逃さないよう注意する．

⑫ヒステロスコープ先端を病変部に進めて，表層の形態的性状を観察する．子宮体癌に関しては，子宮内膜の不整肥厚や腫瘤の存在に注意する．病変部の色調，凹凸不整，びらん，出血，壊死，血管増生，蛇行，奇異に拡張する異型血管の有無が，また腫瘤形成ではポリープ状，結節状，乳頭状，易出血性か，などが良・悪性判定の参考になる．

⑬観察終了後，ヒステロスコープを抜去し，確認した病巣の狙い生検を行う．ヒステロスコープの抜去に続き超音波検査(ultrasonohysterography)を

すると，病巣が容易に描出されるため，掻爬方向の参考になる．

⑭処置用ヒステロスコープの準備があれば，直視下に専用鉗子で主病巣を生検する．

⑮検査終了時に腟内を消毒し，経口抗菌薬を数日間投与する．

6）ヒステロスコピー後のフォロー（図82）

- 子宮内膜増殖症などの広範囲の病巣は，異型増殖症複雑型や子宮体癌の存在を否定するために，子宮内膜全面掻爬を行う．
- 腫瘤全体の病理組織検査が必要なときは，あらためてレゼクトスコープによる経頸管的腫瘍切除術（TCR）を行う．
- 悪性が疑われる子宮壁内（筋層内）発育腫瘤で，内膜面に病変の露出がないときは，腫瘤の針生検を考慮する．
- 子宮頸部，内膜細胞診で悪性細胞が出現し，ヒステロスコピーで異常がないときは子宮外病変の探索が必要である．ヒステロスコピーを含めた子宮内外の定期的検査が重要である．

7）子宮体癌を見逃さないために

- 臨床症状や子宮がん検診などで子宮体癌を疑うときは，ヒステロスコピーを活用し早期診断に努める．
- 初回の検査で異常所見を認めなくても，定期的にヒステロスコピーを含めた検査を行う．
- 自施設で診断がつかないときは，ヒステロスコピーが可能な専門施設へ紹介する．

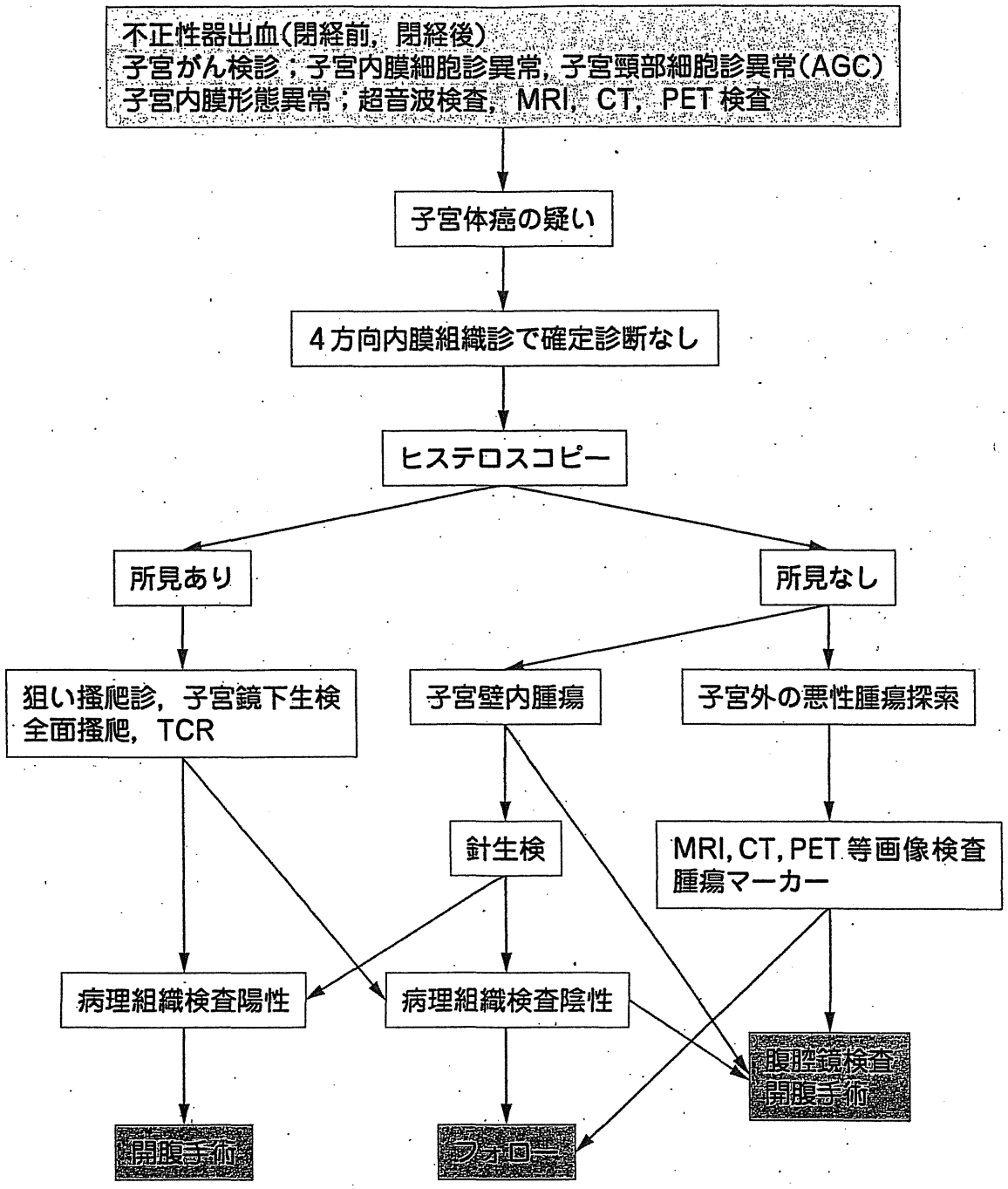

図 82. ヒステロスコピー後の流れ